



## **THERMAL CONDUCTIVITY IN RELATION TO POROSITY AND GEOLOGICAL STRATIGRAPHY**

**Salima Ouali**

CDER – Center for Development of Renewable Energies of Algeria  
P.O. Box 62, Route de l'Observatoire  
Bouzareah, Alger  
ALGERIA  
*waali07@yahoo.fr*

### **ABSTRACT**

Thermal conductivity of rocks is one of the most important parameters in thermal studies of geothermal features. The best estimation of heat quantity and heat flow of geothermal systems depends on accurate calculations of thermal conductivity in porous media. Several authors have studied thermal conductivity and have found it to be connected to several parameters including rock porosity, the most influential parameter.

The aim of this project is to analyse small scale variations in thermal conductivity in context with porosity and the stratigraphic column. High resolution temperature logs were made for this project in well HS-36 located in Reykjavík, SW-Iceland. A detailed study focusing primarily on the depth between 400 and 600 m was completed. The temperature gradient was studied where the vertical heat flow is constant and does not have a horizontal component. The results obtained show that thermal conductivity decreases with increasing porosity and the relationship between thermal conductivity and porosity is close to the harmonic average theoretical equation.

The relationship between resistivity and porosity was also studied. The results from HS-36 were relatively close to a theoretical curve when a scale factor was applied.

### **1. INTRODUCTION**

The main purpose of this project is to investigate if variations in thermal conductivity of Icelandic rock can be analyzed by using high resolution temperature logs and to study the relationship between thermal conductivity and porosity. To do this, special geophysical logs were run in a 1000 m deep well in Reykjavík (HS-36). This well was selected since it is known to be in a thermal equilibrium; the well has not been disturbed by pumping or recent logging and vertical heat flow is dominant in the lower part of the well.

This work includes the following main steps:

1. A brief presentation of the study area and its geological and geothermal context;

2. A general background for the project including a presentation of theoretical equations used for comparing the results (thermal conductivity – porosity equation, resistivity – porosity equation);
3. An explanation of field measurements and data processing carried out during the work;
4. A discussion of the results and interpretation.

## 2. BACKGROUND

### 2.1 Location and geology of study area

Geothermal areas in Iceland are divided into high- and low-temperature areas. High-temperature areas reach temperatures higher than 200°C at 1 km depth and are located within a zone of rifting and volcanism; low-temperature areas have temperatures less than 150°C at the same depth (e.g. Axelsson, 1991). They are all located outside the active volcanic zone. The regional heat flow in Iceland (Fridleifsson, 1979) varies from about 80 mW/m<sup>2</sup> (furthest away from the active volcanic zones crossing the country) to about 300 mW/m<sup>2</sup> in some regions at the margins of the Reykjanes – Langjökull axial rift zone.

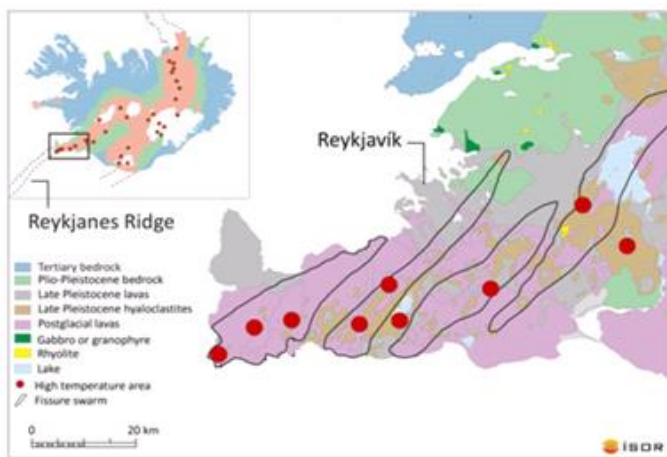


FIGURE 1: Simplified geological map of the Reykjavik area (ISOR- database)

Due to its geographical location across the Mid-Atlantic Ridge, Iceland is characterised by intense tectonic, volcanic and geothermal activities. The Reykjavik area is located in SW-Iceland (Figure 1). According to a geological study of this region (Tómasson et al., 1975), this thermal area is in Quaternary volcanics characterised by thick successions of low-porosity lavas, intercalated by high-porosity, subglacial volcanics, which form ridges tens of kilometres long. The stratigraphy of the thermal fields ranges in age from about 2.8 to 1.8 My. There are signs of ten glaciations in the volcanic succession.

During this time span there were two central volcanoes active in the region, the Kjalarnes (which is older) and the Stardalur central volcanoes. This resulted in a thick accumulation of hyaloclastites in the vicinity of the volcanoes.

### 2.2 Reykjavik geothermal fields

Geothermal drilling in Reykjavik started in 1928, when shallow geothermal wells were drilled in low-temperature fields for hot water. Reykjavik has utilized three low-temperature fields located in Laugarnes, Ellidaár, and Mosfellssveit and one high-temperature field (Nesjavellir) (Gunnlaugsson and Gíslason, 2003). The energy produced from these fields is mainly used for district heating. Electricity is also provided from the Nesjavellir power plant. Another high-temperature geothermal field in the vicinity of Reykjavik, the Hellisheidi field, has been explored by Reykjavik Energy and electricity production was recently (2006) initiated from the Hellisheidi power plant. In Reykjavik all houses are heated at present by geothermal energy and the capital is considered to be one of the cleanest in the world.

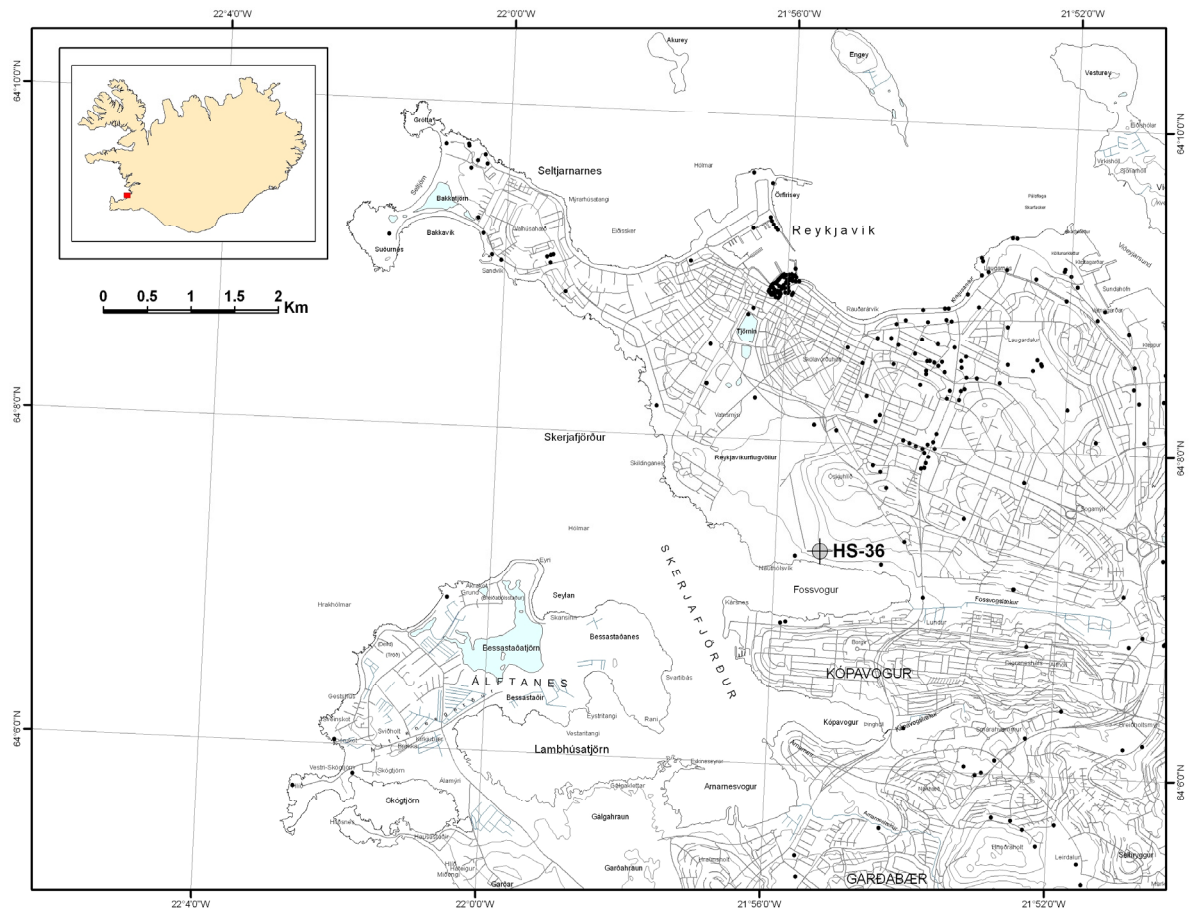


FIGURE 2: Location of well HS-36 in Nauthólsvík in the Reykjavík area (ISOR - database)

### 2.3 Stratigraphy of well HS-36

Well HS-36 (Figure 2) is an exploration well that Reykjavík Energy drilled in Nauthólsvík, in the southern part of Reykjavík in October 1993 to investigate the temperature at the edge of the Laugarnes area and the pressure effects due to utilization in the area (Tómasson, 1983). It is a low-temperature well with an average temperature gradient of  $46^{\circ}\text{C}/\text{km}$ . The borehole stratigraphy shown in Figure 3 represents the main lithological layers of well HS-36 between 400 and 600 m; it consists primarily of alternating sequences of hyaloclastite units and basaltic layers. The data were provided by ISOR. The following stratigraphic descriptions (Figure 3) are translated from Tómasson (1983):

**408-424 m:** Medium coarse crystallized basalt partly altered with very few fillings. This could be olivine basalt layers and possibly dykes.

**424-464 m:** Hyaloclastite, mainly pure tuff. The upper part is partly crystallized, possibly basalt at the top. The hyaloclastite is considerably altered and all the glass is altered into green palagonite and/or to green smectite and the glass is partly reddish in colour.

**464-484 m:** One or two layers of basalt with small grains at the top and gradually bigger grains farther down, altered at the top.

**484-524 m:** Hyaloclastite, penetrated by one basalt layer, probably a dyke.

**524-588 m:** Basalt layers, the scoria in the basalt layers are marked in Figure 3 as glassy basalt or as basalt rich breccia.

**588-610 m:** Vesicular tuff where the crystal size is smaller than the cutting size (tuffaceous sediment).

**2.4 General information about well logging**

A brief description of the important well logs used here, taken from "Geothermal logging I" by Stefánsson and Steingrímsson (1990), is given below.

*Temperature log*

The fundamental parameter in geothermal investigation is temperature which is measured with a thermometer which records the signal down and up the well. The temperature measurements are recorded continuously and the temperature logs record temperature with depth.

*Natural gamma ray well log*

These logs record the radiation due to the presence of radioactive-isotopes in geological succession (<sup>40</sup>K, <sup>238</sup>U, <sup>232</sup>Th). The important isotopes are found in small quantities in rocks. The standard calibration unit is *API Gu* (American Petroleum Institute Gamma units).

*Neutron-neutron well log*

Neutron-neutron logs are used in porosity investigation. The neutron log tool consists of a neutron source (Americium-Beryllium). The emitted high-energy neutrons collide with the hydrogen on their way from the source to the detector and the lower-energy thermal neutrons are detected by the counter, i.e. the detector of the instruments. The recorded log indicates the ability of the formation to slow down the fast neutrons; this ability is primarily controlled by the abundance of hydrogen which is mostly found in fluid formations. A standard calibration unit *API Nu* is used (American Petroleum Institute Neutron units).

*Resistivity well log*

Resistivity logs are of great importance in geothermal investigation because of the difference in electrical properties between different formations. The resistivity log shows lithological variation clearly. There exist many types of resistivity logs. Stefánsson and Steingrímsson (1990) described the normal log which was used in this study:

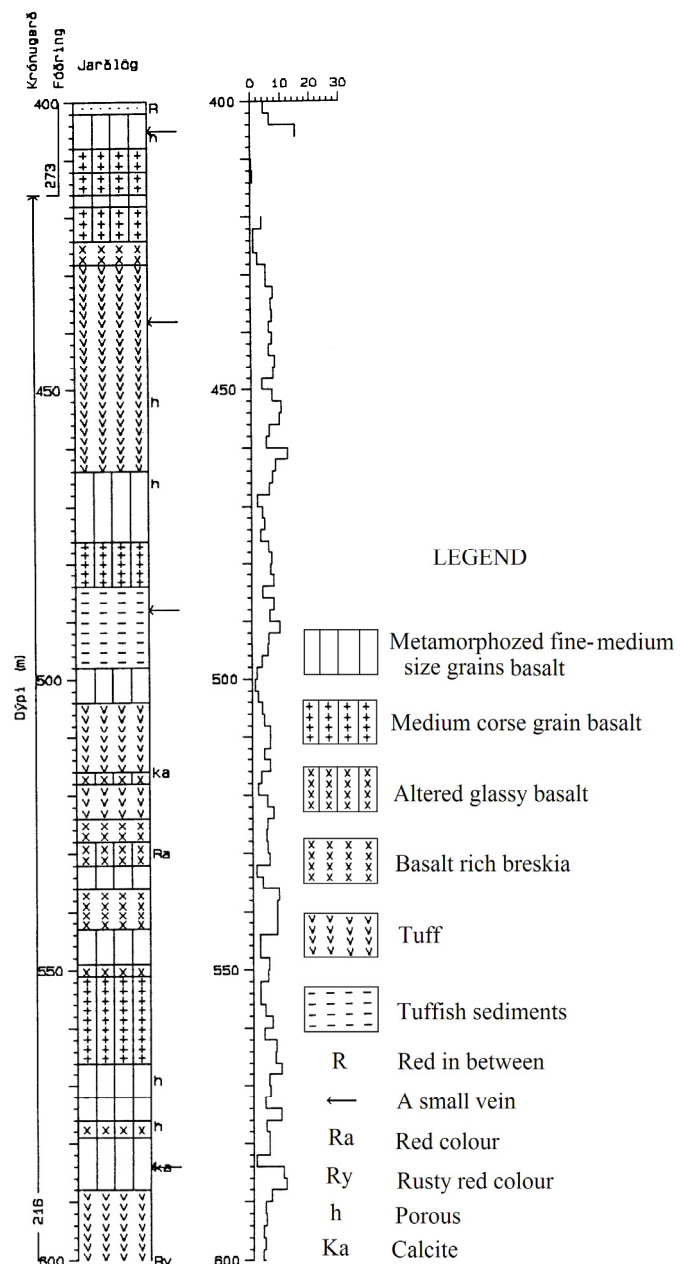


FIGURE 3: Stratigraphic column of well HS-36 (Tómasson, 1983)

“The normal resistivity log is a four-electrode array with two electrodes fixed on the logging sonde in the well. The third electrode is placed at the surface, but the armour of logging cable is usually used as the fourth electrode. During logging a constant current  $I$  is driven between the electrode on the sonde and the cable armour, and the voltage  $V$  between electrodes  $M$  and the surface electrode  $N$  is measured. For the normal electrode array the resistivity of an infinite homogeneous medium is given by the relation:

$$\rho = 4 \pi \overline{AM} \frac{V}{I} \quad (1)$$

where  $\overline{AM}$  = The distance between the two electrodes fixed on the logging sonde.

In oil well logging the standard values used for  $\overline{AM}$  spacing are:

$$\overline{AM} = 16'' \text{ and } 64''$$

In a non-uniform medium, the resistivity defined by the above relationship is the apparent resistivity; the normal resistivity will show the apparent resistivity variations of the medium surrounding the sonde, and will, therefore, include the well itself. The determination of the true rock resistivity will therefore include elimination of well effects (fluid resistivity and well size) as well as the effects of limited bed thickness of the adjacent lithological units. Resistivity logging can only be done in the uncased part of the well below water level.” According to Stefánsson and Steingrímsson (1990), the maximum operation temperature is 150-200°C depending on cable and cablehead used, whereas for safety the limits are 130-150°C.

#### *Caliper well log*

The caliper log is fundamental in geothermal exploration since it records the diameter of a well. The diameter of a well is directly related to the nature of the formations crossed.

### **2.5 Previous temperature logs in HS-36**

A total of 16 temperature logs had been measured in well HS-36 from the initiation of the drilling (Figure 4a) until the project presented in this paper was initialized. The first temperature measurements were carried out at the end of drilling the first section of the well in October 1995. The temperature logs in Figure 4b show a stable temperature state reflecting the true rock temperature i.e. the temperature after the effects of drilling had relaxed. The stable temperature profiles show a very high temperature gradient near the surface, lowering with depth until it stabilizes at 0.046 °C/m below 400 m depth. The annual average surface temperature of the area is between 4 and 5°C. The bottom hole temperature is 88°C at 1 km depth. This type of temperature profile is typical for wells drilled close to convective geothermal systems.

### **2.6 Heat transfer**

As introduced by Beardsmore et al. (2001), the internal heat is derived both from primordial sources related to the formation of the globe and from secondary processes generating heat internally. The internal heat sources are not distributed uniformly throughout the globe. Of the heat observed flowing out through the earth’s surface, 40% actually originates within the thin outer crust. The heat of radioactive isotopic decay forms the dominant part, but there are also contributions from the friction of intraplate strain and plate motions, and heat from exothermic metamorphic and diagenetic processes. Heat exchanges are thermal transfer phenomena in the earth; they occur in three ways:

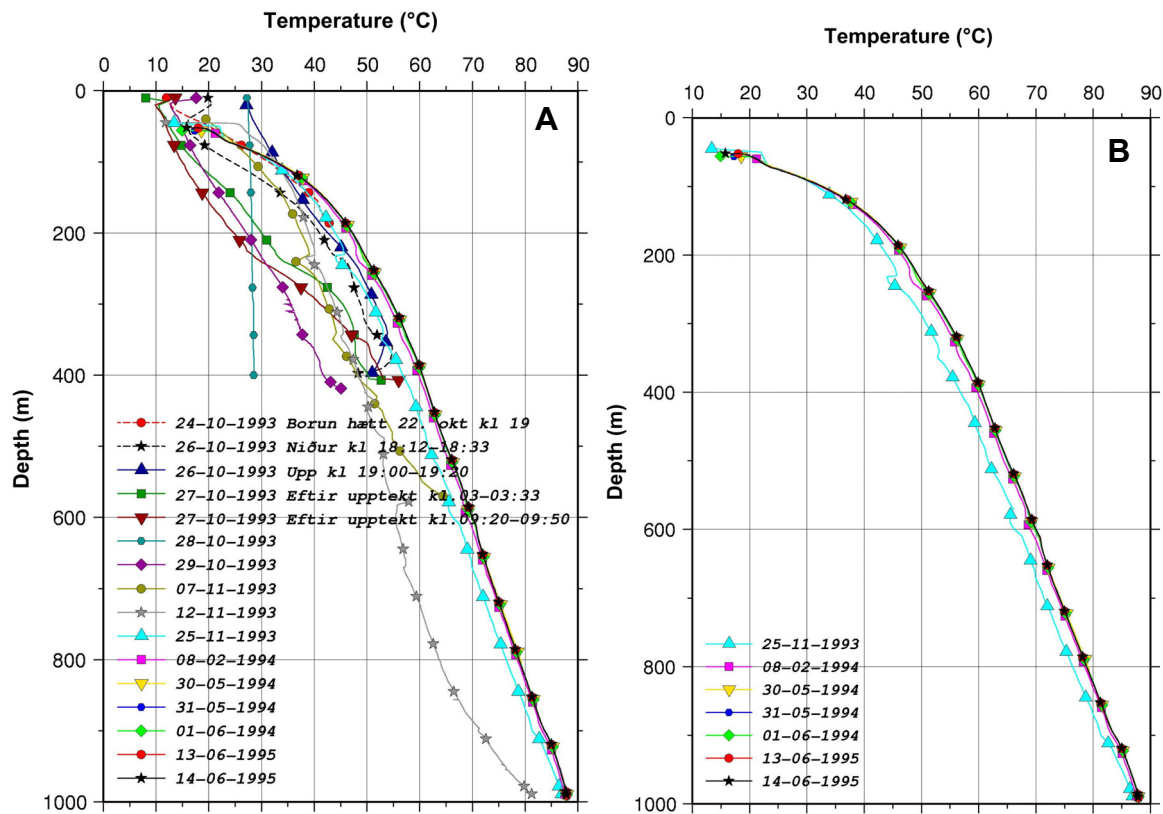


FIGURE 4: HS-36; a) Temperature profiles made in 1993-1995; b) Selected temperature profiles (ISOR-database, Reykjavik Energy)

Conduction governs the transfer of heat in the surface parts of the earth (crust) by atomic vibrations through a material without mass movement. Hersir and Björnsson (1991) stated that in the absence of mass movement the linear relationship between conductive heat flux density  $\vec{Q}_{Cond.}$  ( $Wm^{-2}$ ) and the thermal gradient  $\nabla T$  ( $^{\circ}C m^{-1}$ ) can be written in a general form as:

$$\vec{Q}_{Cond.} = -K\nabla T \tag{2}$$

where  $\vec{Q}_{Cond.}$  = Total heat flux [ $Wm^{-2}$ ];  
 $K$  = Thermal conductivity [ $Wm^{-1}^{\circ}C^{-1}$ ];  
 $T$  = Temperature [ $^{\circ}C$ ].

Since the heat flow in the earth's crust is mainly vertical, it can be approximated by:

$$\vec{Q}_{Cond.} = -K \frac{dT}{dZ} \tag{3}$$

where  $Z$  = The depth coordinate, i.e. down into the earth.

Convection governs the transfer of heat in deeper parts of the earth (mantle and core) within many geothermal systems. This transfer mode includes the transport of energy by mass movement, by fluid in geothermal systems and magma or ductile material in the Earth's mantle. There are two types of convections, free or natural convection, in which the movement of fluid is due to changes in density and forced convection in which the movement of the fluid is imposed by external pump ventilation.

In radiation, heat is transferred between two bodies by electromagnetic waves or radiation. This kind of heat transfer only happens at very high temperatures and is not encountered in geothermal systems.



The thermal conductivity of rocks is quite variable according to rock type (Table 1); it varies commonly from  $1.2 \text{ Wm}^{-1}\text{C}^{-1}$  in porous volcanic tuffs to more than  $4.0 \text{ Wm}^{-1}\text{C}^{-1}$  in silica rich formations.

TABLE 1: Thermal conductivity of various rocks at room temperature (Rybach, 1981)

Rock type	Thermal conductivity (W/m°C)
Dolomite salt	5.0
Peridotite/pyroxenite	4.2-5.8
Granite	2.5-3.8
Limestone	1.7-3.3
Gabbro /basalt	1.7-2.5
Sandstone	1.2-4.2
Volcanic tuffs (depending on porosity)	1.2-2.1
Shale (depending on water content)	0.8-2.1
Deep sea sediments (depending on water content)	0.6-0.8
Water	0.6

Heat flow measurements are commonly taken in geothermal exploration, necessary in order to calculate heat flow data from temperature gradient as well as thermal conductivity. If the thermal conductivity can be regarded as constant through the well, it is not necessary to measure the thermal conductivity since it is time consuming and needs rock samples, preferably cores. In Iceland it has been assumed that the variations in thermal conductivity are so small that they can be discarded and the gradient is used instead of heat flow. This approach cannot be used in continental areas or sedimentary basins due to the variability in thermal conductivity.

## 2.7 Porosity of rocks

Porosity is the fraction of the total volume of rock that is not occupied by the solid constituents (Serra, 1984). There are several kinds of porosity. The total porosity,  $\phi_t$ , consists of all the void spaces (pores, channels fissures, vugs) between the solid component. It is either represented as percentage or fraction.

$$\phi_t = \frac{V_t - V_s}{V_t} = \frac{V_p}{V_t} \quad (4)$$

where  $V_p$  = Volume of all the empty spaces (generally occupied by oil, gas water) [ $\text{m}^3$ ];  
 $V_s$  = Volume of the solid materials [ $\text{m}^3$ ]; and  
 $V_t$  = Total volume of rocks [ $\text{m}^3$ ].

Porosity is a fraction between 0 and 1 (or 0-100%). Typically it ranges from less than 0.01 for solid granite to more than 0.5 for coarse grained unconsolidated material.

Figure 5 shows two types of pores, i.e. fractures and interconnected pores, usually named fracture porosity, and closed pores.

The total porosity is the sum of both. Effective porosity is that fraction of pores that can contribute to fluid flow and is usually close to or a little bit less than the fracture porosity.

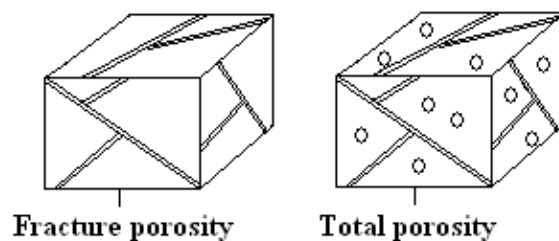


FIGURE 5: Fracture and total porosity

## 2.8 Relationship between thermal conductivity and porosity

As referred to by Stefansson (1997), the thermal conductivity of rocks is highly dependent upon porosity. The variation in thermal conductivity measurements for various different rock types (Cermák and Rybach, 1982) is largely due to the variation in porosity of the rock samples measured. Some authors have pointed out the effects of porosity on the thermal conductivity of rocks. It has been specified in Beck's study (1976) that four main empirical equations should mostly be used: Parallel coupling of the components (weighted average) (Equation 5); Serial coupling of the components (weighted harmonic average) (Equation 6); Geometrical average (Equation 7) and Dispersive model (Maxwell's equation) (Equation 8). Three of these equations have been the subject of a study by Stefansson (1997) in order to define the best equation describing the relationship between thermal conductivity and porosity. He based his study on the four relationships in Equations 5-8 using thermal conductivity measurements from Icelandic basalt samples, as well as two data sets from Mexico and sandstone from Cajon Pass in USA. The results showed that the geometrical average (Equation 7) provided the best relationship. In Equations 5-8 the following nomenclature applies:

$$\begin{aligned} \phi &= \text{Porosity, here as fraction;} \\ K &= \text{Thermal conductivity [Wm}^{-1}\text{°C}^{-1}\text{]}; \\ K_w &= \text{Thermal conductivity of water [Wm}^{-1}\text{°C}^{-1}\text{]}; \\ K_r &= \text{Thermal conductivity of rock matrix [Wm}^{-1}\text{°C}^{-1}\text{]}; \text{ and} \\ r = \frac{K_r}{K_w} &= \text{The ratio between the thermal conductivity of the rock matrix and water.} \end{aligned}$$

*The weighted average or linear equation:*

$$K = \phi K_w + (1 - \phi)K_r \quad (5)$$

*The harmonic average equation:*

$$\frac{1}{K} = \frac{\phi}{K_w} + \frac{(1-\phi)}{K_r} \quad (6)$$

*The geometrical average equation:*

$$\log K = \phi \log K_w + (1 - \phi) \log K_r \quad (7)$$

*Maxwell's equation:*

$$K = K_r \left( \frac{(2r + 1) - 2\phi (r - 1)}{(2r + 1) + \phi (r - 1)} \right) \quad (8)$$

Equations 5 and 6 are used in the comparison of the data in this study (Section 4.6).

## 2.9 Relationship between resistivity and porosity

Flóvenz et al. (1985) studied the large scale relationship between resistivity, porosity and temperature based on an analysis of results from geophysical exploration data. They modified the double-porosity model proposed by Stefansson et al. (1982), and added the effects of interface conductivity. The modified equation is:



$$\frac{1}{\rho} = \frac{0.22}{\rho_w} \left( 1 - (1 - \phi_f)^{\frac{2}{3}} + \frac{(1 - \phi_f)^{\frac{2}{3}}}{1 - (1 - \phi_f)^{\frac{1}{3}} + (1 - \phi_f)^{\frac{1}{3}} 4.9 \times 10^{-3}} \right) + \frac{\phi_f^{1.06}}{b} \quad (9)$$

where  $\rho_w = \rho_{wo}/[1 + 0.023(T - 23)]$ ;  
 $b = 8.7/[1 + 0.023(T - 23)][1 + 0.018(T - 23)]$ ;  
 $\rho =$  Resistivity of the rocks [ $\Omega\text{m}$ ];  
 $\phi_f =$  Fracture porosity, here as a ratio;  
 $\rho_w =$  Resistivity of fluid in the rock matrix [ $\Omega\text{m}$ ];  
 $\rho_{wo} =$  Resistivity of fluid in the rock matrix, at reference temperature  $T_o$  [ $\Omega\text{m}$ ];  
 $T =$  The in-situ temperature [ $^{\circ}\text{C}$ ].

Flóvenz et al. (1985) furthermore show that in the case of low-salinity pore fluid like in most low-temperature geothermal fields in Iceland, the bulk resistivity is almost independent of the pore fluid resistivity. This is due to the effect of interface conduction of clay minerals in the pores. Therefore the first item of Equation 9 can be discarded and the equation reduces to:

$$\frac{1}{\rho} = \frac{\phi_f^{1.06}}{b} \quad (10)$$

### 3. BOREHOLE LOGGING AND RECORDING OF DATA

#### 3.1 Borehole logging

Various types of loggings were carried out during August 10-11, 2009 in well HS-36 in Nauthólsvík. The well is vertical and 1000 m deep, and located at the edge of the Laugarnes low-temperature field. Figure 6 shows the well, the logging truck doing field measurements and the data acquisition system. The first recording was a temperature log, starting at 4 m depth and finishing at 989.7 m depth. The water level was reached at 36 m depth. Continuous data were recorded on a WARRIOR recorder with depth resolution up to  $\Delta z = 0.076$  m for the temperature log. The other measurements used in this study: resistivity, caliper, neutron and gamma logs were done with a resolution of  $\Delta z = 0.2$  m. Older measurements were recorded using the NIMBIN software which has less resolution.

#### 3.2 The initial data processing

Data used in this study are recorded in digital files and are processed at ISOR – Iceland GeoSurvey using several programs on a Unix mainframe computer. The data processing includes some corrections such a depth correction (0-reference point), and correcting resistivity for the influence of width, temperature and fluid in the well.

**Depth correction:** After the measurements, the recorded data may show small inconsistencies in the depth scale. By doing a depth correction, the data will become more consistent. It is possible to correct the depth in the caliper log by comparing the measured profile with the known casing depth and based on that correct the depth in the caliper file. Afterwards, it is possible to compare or correlate the neutron-neutron (NN) and resistivity with the corrected caliper log and, with respect to each other, find the offset in depth to be used to correct each of them. The gamma log is measured with NN so it can be corrected in context with the NN-depth correction.

While drilling a borehole the measurements refer to the drilling floor (platform); later the measurements refer to the surface. Therefore, it may be necessary to correct the depth when comparing data from different periods. A comparison of the well logs could aid in the depth correction process.

**Resistivity correction:** The resistivity logs (16" and 64") were corrected for the influence of the temperature, and the fluid in the well and the caliper of the well using software to read the resistivity, temperature and caliper logs. The caliper log is used to find how much fluid is around the instruments in the well; the resistivity of the water in the well is assumed to be 55  $\Omega$ m in the calculations.

**Porosity calculations from neutron-neutron measurements:** The porosity calculations gave high values in this study. A well having a diameter 9" or 229 mm is at the upper limit of calibration for the porosity calculations. The width of HS-36 is larger. Therefore, the results were not reliable although extrapolation was used to extend the limits of the calculations. When the values of the caliper log are outside the limits of the software, the result is a 0-value which signifies: "Cannot be calculated". On the other hand, the output-values could be useful as relevant values with respect to each other.

## 4. RESULTS AND DISCUSSIONS

### 4.1 Temperature log

The temperature profile of HS-36 was plotted using the ORIGIN software. The profile (Figure 7) shows, as expected, the same overall results as the previous temperature profiles (Figure 4), but the new profile was measured with a higher resolution than previously. Small disturbances in the temperature profile may be noticed at approximately 610 and 900 m depth. This might be explained by small aquifers at these depths with slow movement of water from 610 to 900 m. For this study it was necessary to analyse a well or a portion of a well with stable vertical heat flow and no fluid movement. Therefore, the depth interval of 400-600 m was selected.



FIGURE 6: Data acquisition system; 1) Logging truck; 2) Logging equipment; 3) Well HS-36

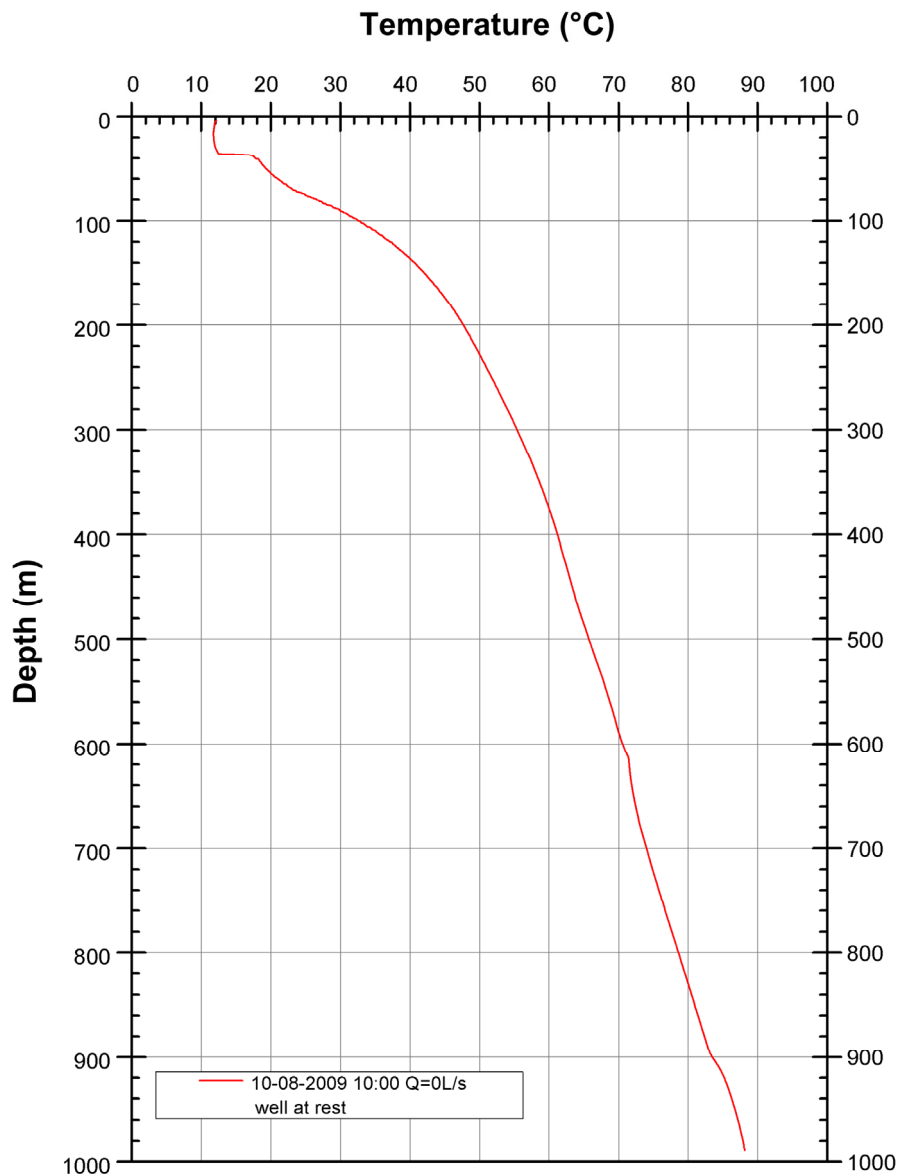


FIGURE 7: Temperature profile from well HS-36, measured in August 2009

#### 4.2 Temperature, caliper and lithological logs

Temperature, caliper, resistivity, NN and gamma logs as well as calculated porosity were plotted using the ORIGIN software, allowing an exact comparison between the different well logs. Figure 8 shows the well logs including the temperature profile at the 400-600 m depth interval which was chosen for the detailed study of the temperature profile. These include the temperature profile together with the caliper logs, corrected resistivity, NN, calculated porosity and gamma. Figure 9 is a very detailed plot of the temperature log in the same depth interval. It may be noticed that here the temperature gradient is rather stable. From this graph seven smaller depth intervals were selected with a relatively stable temperature gradient within each one of them. For these minor intervals the well logs in Figure 8 were analysed in detail. The main results are shown in Table 2. Here, Figures 10, 12 and 13 have been used for an estimation and calculation of the averages for the porosity, resistivity, thermal conductivity and thermal gradient for the selected depths intervals shown in Table 2. In the following sections the processing of each type of data is explained.

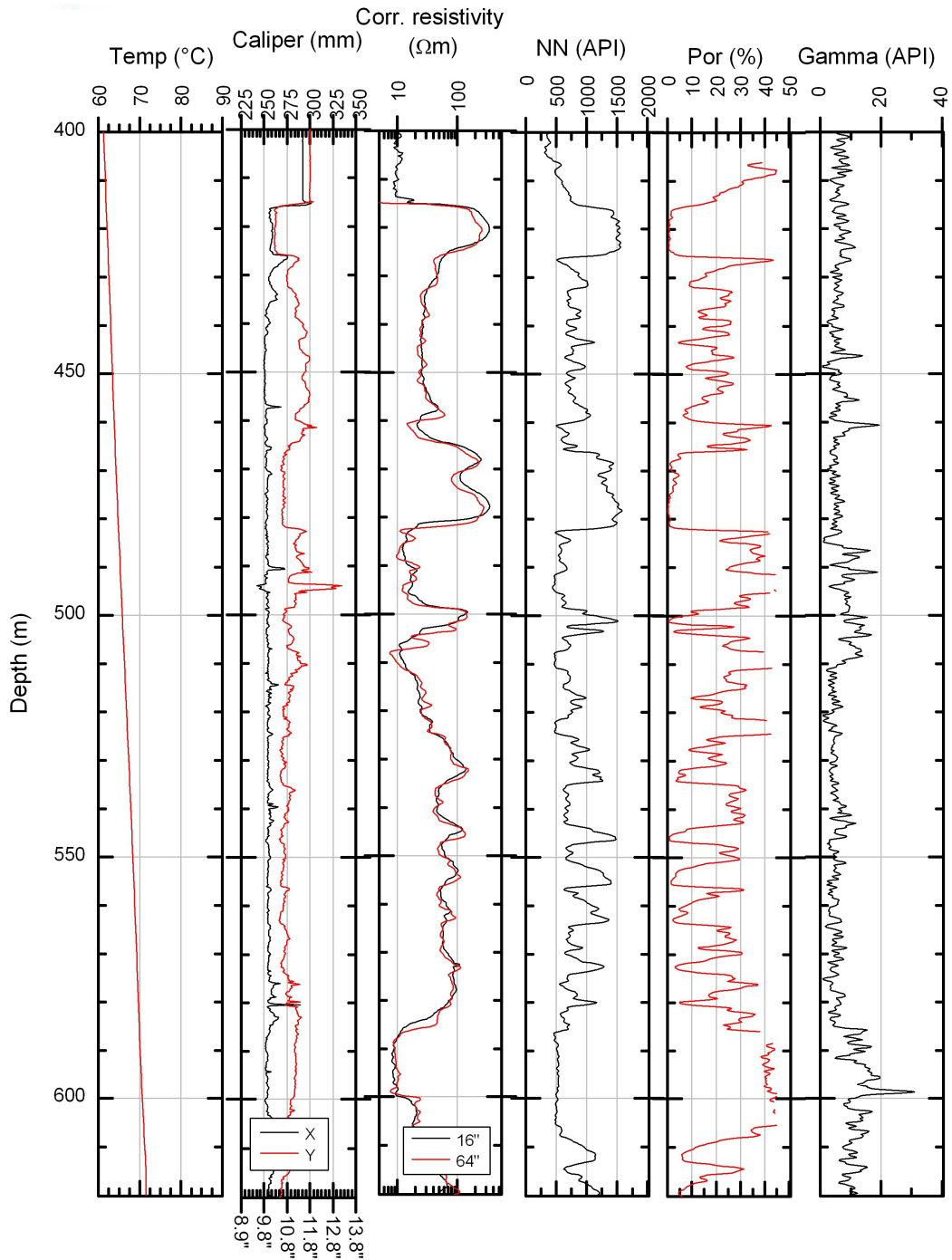


FIGURE 8: Temperature, caliper, corrected resistivity, NN and gamma logs in well HS-36 from 400 to 640 m, measured in August 2009, as well as calculated porosity

### 4.3 Data of thermal gradient from well HS-36

In order to observe variations in the temperature gradient, it was necessary to calculate the gradient directly from the measurements as no obvious small scale variations could be seen in the logs from 400 to 600 m depth in well HS-36. The thermal gradient in high resolution was used to identify intervals where there were relatively small changes in the temperature gradient.

Figure 10 shows the calculated temperature gradient between 400 and 600 m. The gradient is calculated by a 3 point running average of the measured temperature which gives the average

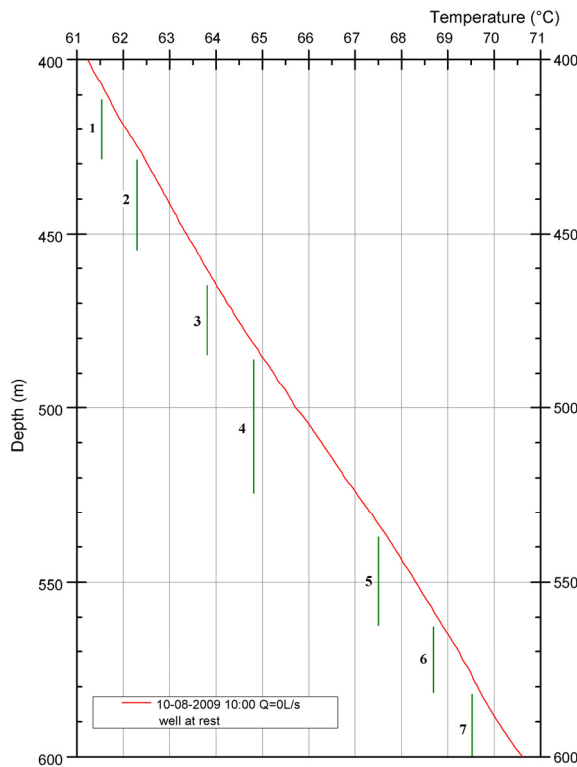


FIGURE 9: Detailed temperature profile from 400 to 600 m in HS-36; the seven depth intervals selected for special studies are shown

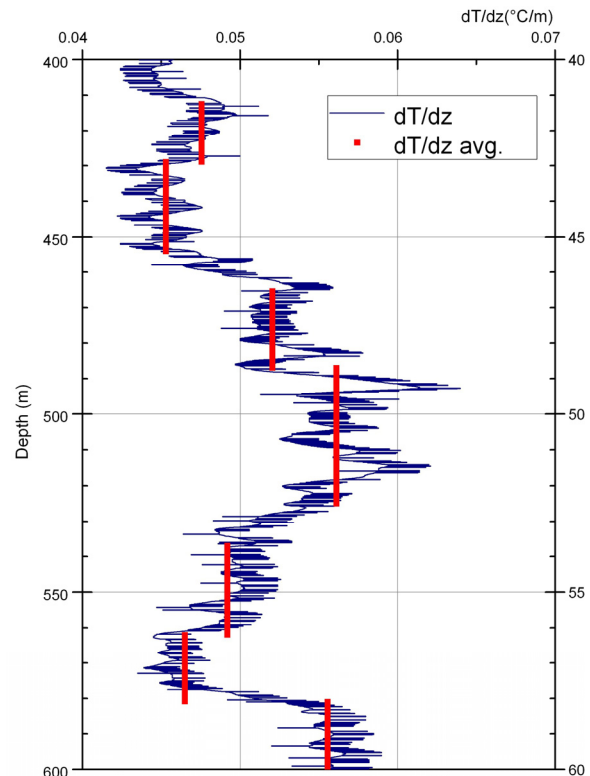


FIGURE 10: The calculated thermal gradient vs. depth in the 400-600 m interval in HS-36 and average values for the seven selected depth intervals

gradient over every 15 cm interval. Figure 10 shows clearly that there are relatively large small scale variations in the temperature gradient with depth.

TABLE 2: The average porosity, resistivity, thermal conductivity and thermal gradient of HS-36 for the seven selected depth intervals

No.	Depths intervals [m]	Average porosity [%]	Average resistivity [ $\Omega$ m]	Average thermal conductivity [ $\text{Wm}^{-1}\text{°C}^{-1}$ ]	Average $dT/dz$ [ $\text{°Cm}^{-1}$ ]
1	412-429	11.2	173	1.97	0.04755
2	429-454	18.8	28.5	2.06	0.04527
3	465-487	10.9	169	1.80	0.05204
4	487-525	29.8	30	1.67	0.05611
5	537-562	20.3	69	1.90	0.04919
6	562-581	18.9	75	2.01	0.04649
7	581-600	39.0	15	1.69	0.05555

#### 4.4 Average thermal gradient – average thermal conductivity

To calculate the thermal conductivity as a function of depth, the following method was applied: The typical value of the thermal conductivity for Icelandic basaltic rocks (Flóvenz and Saemundsson, 1993) is close to  $1.8 \text{ Wm}^{-1}\text{°C}^{-1}$ . By using this for K in Equation 3, assuming it is the average thermal conductivity for the depth interval 400-600 m in HS-36 and using the average thermal gradient from this depth interval in the well,  $0.052 \text{ °Cm}^{-1}$ , the vertical heat flow

of  $0.0936 \text{ Wm}^{-2}$  was calculated. This was, in turn, used to get the results for the thermal conductivity for each of the 7 depth intervals using the thermal gradient for each of them.

The graphs in Figures 10 and 11 show the calculated and average thermal gradient and calculated and average thermal conductivity in the selected depth intervals. The thermal conductivity values were calculated for the average temperature gradient values corresponding to the 7 selected depth intervals. Using the formula of heat flux by conduction (Equation 3) the thermal conductivity was calculated, assuming that the vertical heat flow is constant between 400 and 600 m depth, at  $0.0936 \text{ Wm}^{-2}$ .

It may be noticed on these graphs that the thermal gradient varies inversely to thermal conductivity with depth, easily seen by looking at Equation 3. The lowest thermal gradient value was observed in the second depth interval,  $0.04527 \text{ }^\circ\text{C/m}$ , and the highest value was found in the fourth depth interval,  $0.05611 \text{ }^\circ\text{C/m}$ . The corresponding thermal conductivity values were, respectively,  $2.06 \text{ Wm}^{-1}\text{ }^\circ\text{C}^{-1}$  and  $1.67 \text{ Wm}^{-1}\text{ }^\circ\text{C}^{-1}$ .

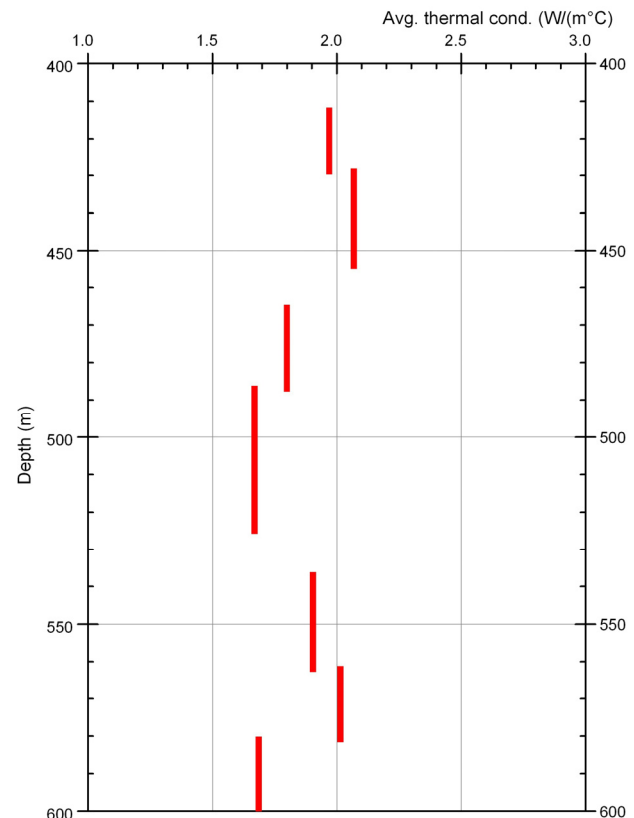


FIGURE 11: The seven selected average thermal conductivity values in the 400-600 m interval in HS-36

#### 4.5 Porosity and resistivity

The neutron-neutron measurements were used to calculate the porosity according to a model which only shows relative results for HS-36, due to the too large diameter of the well as explained in Section 3.2. The graph in Figure 12 shows the porosity log at 400-600 m depth and the average for each of the pre-selected depth intervals. The graph in Figure 13 shows the corrected resistivity log at 400-600 m depth and the average for each pre-selected depth interval. The average porosity values were higher than expected.

The calculated porosity and the average porosity values shown in Figure 12 highlight that the first three intervals are characterized by lower porosity values than the fourth interval. The porosity in intervals 5 and 6 is close to the porosity in interval 2. The third depth interval shows the lowest porosity and the first one is only a little bit higher. The highest porosity is seen in the seventh interval.

The graph in Figure 13 shows the 64" resistivity log which was corrected for the influence of the width of the well as well as the influence of the temperature and the fluid in the well. The average resistivity values range between 15 and 173  $\Omega\text{m}$ . By comparing the graphs in Figures 12 and 13, it is clearly observed that the highest porosity was detected at the lowest resistivity. The lowest porosity on the other hand was found at the first and third depth intervals, where the highest resistivity values were found as well. The general result is that the resistivity changed inversely to the porosity, as expected.



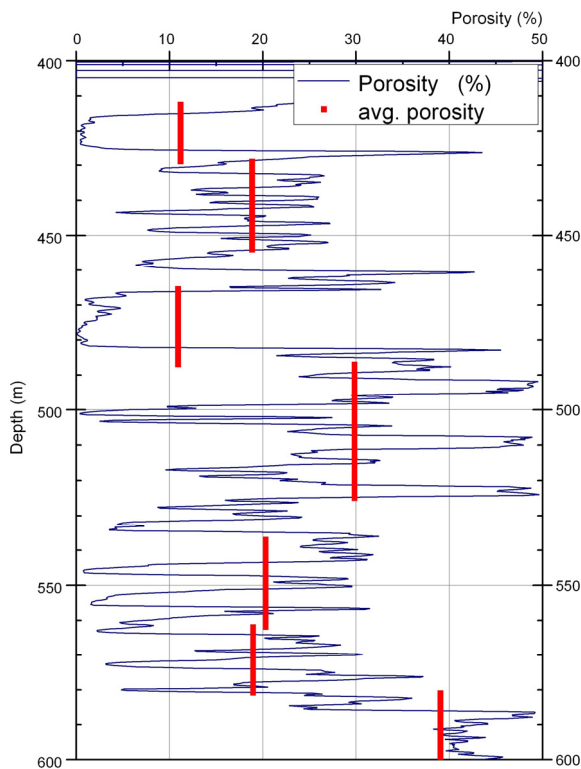


FIGURE 12: The calculated porosity vs. depth in the 400-600 m interval in HS-36 and average values for the seven selected depth intervals

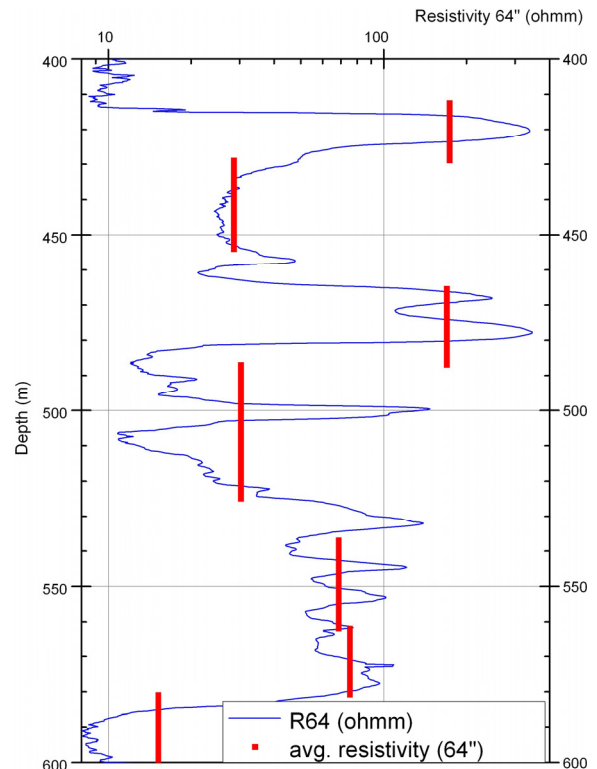


FIGURE 13: The corrected resistivity vs. depth in the 400-600 m interval in HS-36 and average values for the seven selected depth intervals

#### 4.6 Thermal conductivity against porosity

Figure 14 shows thermal conductivity as a function of porosity for the 7 selected intervals in HS-36. It may be noticed in Figure 14 that the thermal conductivity decreased with increasing porosity except for two points which shifted to lower values. They correspond to the first and third depth intervals which are characterized by very low porosity resulting from the high NN-values in these intervals (Figure 8).

In order to compare these data (Figure 15) to the theoretical relationship between thermal conductivity and porosity, two theoretical equations were used, the harmonic average (Equation 6) and the geometric average (Equation 7). The parameters used in these equations are those by Stefánsson (1997):

$$K_w = \text{Thermal conductivity of water} = 0.628 \text{ W/m}^\circ\text{C};$$

$$K_r = \text{Thermal conductivity of rock matrix} = 4 \text{ W/ m}^\circ\text{C}.$$

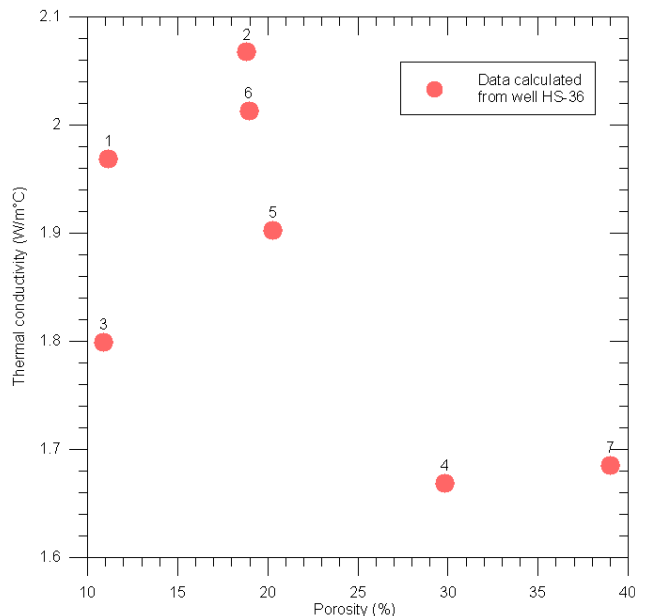


FIGURE 14: Thermal conductivity values vs. porosity for well HS-36



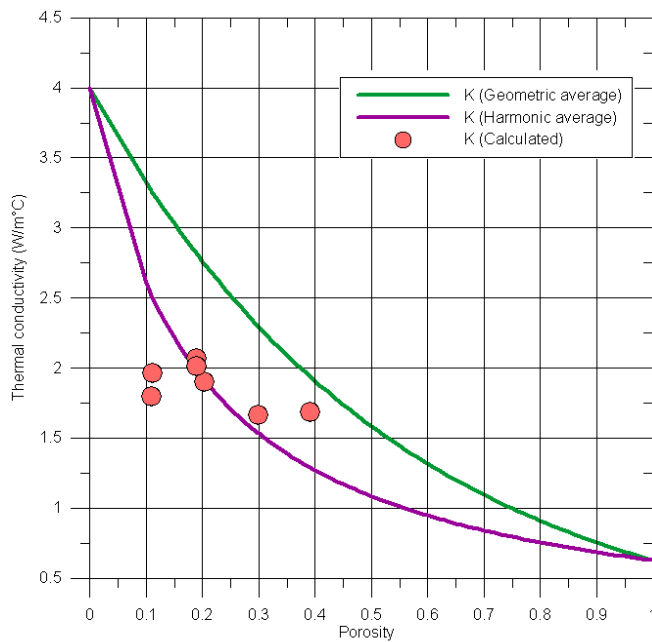


FIGURE 15: Thermal conductivity values vs. porosity for well HS-36 compared with curves from Stefánsson (1997)

The results for well HS-36 fit relatively well to the theoretical curve representing the harmonic average equation (Figure 15).

#### 4.7 Resistivity against porosity

The average resistivity for the seven depth intervals was plotted against the porosity (Figure 16). The resistivity decreases in a fairly regular way with porosity except for interval 2 which has lower resistivity than intervals 5 and 6 which have fairly similar porosity values. The average resistivity corresponds to an interval with average porosity and low resistivity in the upper part of the borehole. In order to compare these results from well HS-36 and the previously tested theoretical relationship (Flóvenz et al., 1985), Equation 9 describing a relationship between

resistivity and fracture porosity was plotted (Figures 17 and 18). The simplified Equation 10 was used with the parameters:

$$b \sim 3.093$$

$$T \sim 67^{\circ}\text{C} \text{ (the average temperature in the layer between 400 and 600 m)}$$

Figure 17 was plotted using a linear scale where the theoretical resistivity data was multiplied by 3.5, in order to check if it could be fitted closer to the real data. Figure 18, on the other hand, was plotted using a logarithmic scale.

The graphs show that the results do not fit too well with the theoretical curve. The best fit of the real data is given by the equation:  $y = 2.797/x^{1.838}$ , where the correlation factor is  $R = 0.82$ . This equation is close to Equation 10 using a scale factor of 3.5 but both graphs (Figures 17 and 18) indicate that after applying a good scale factor to the results, the data fits quite well. Also the forms of the curves in Figure 17 are not far from each other.

The difference in scale between these two sets of data could be partly due to the simplification of Equation 9 to Equation 10, which is used in this study. Another factor affecting the results could be the difference between the fracture porosity used in Equation 5 and total porosity calculated from well HS-36. In

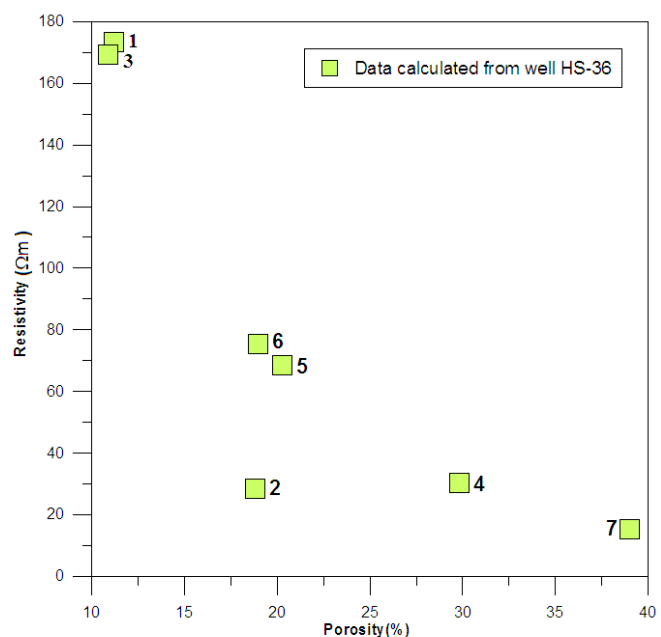


FIGURE 16: Resistivity vs. porosity graph for the seven selected depth intervals in HS-36

addition, a part of the explanation could be a difference in the scales based on the origin of the data, as Equation 9 was based on surface measurements and the results of this study were taken from borehole logs.

## 5. CONCLUSIONS

The thermal conductivity of rocks is clearly influenced by the porosity. From this study it is established experimentally that there is a reduction in thermal conductivity with increasing porosity. The results from HS-36 are close to the harmonic average theoretical relationship between thermal conductivity and porosity.

It is also shown with results from well HS-36 that resistivity decreases with increasing porosity and that the results could be fitted relatively well with a theoretical relationship between porosity and resistivity by taking into account a scale factor for the results from HS-36.

For further studies of the thermal gradient it would be of interest to measure well logs where an exact geological succession is known. Using selected geological layers in correlation with lithological logs, where the temperature gradient is relatively stable, could possibly give more precise results.

## ACKNOWLEDGEMENTS

It is with great pleasure that I wish to thank all those with whom I have shared the 6 month training period at UNU-GTP. I would like to express my thanks and my gratitude to Dr. Ingvar Birgir Fridleifsson, Director of UNU-GTP, for creating a cordial work environment, and for the excellent training programme we had. My respectful thanks go to Mr. Lúdvík S. Georgsson, Deputy Director of UNU-GTP, for a very well organised training programme and for moral support and help. I would like to express my great acknowledgement of my supervisor Ms. Svanbjörg Helga Haraldsdóttir from whom I have learned a lot, for advising and guiding me so well. I am deeply indebted to Dr. Ólafur G. Flóvenz, for proposing the theme for this study and for assistance and supervision for the proper completion of the project. My thanks and appreciation go to all the staff of UNU-GTP, Ms. Dorthe H. Holm, Ms. Thórhildur Ísberg, Mr. Markús A.G. Wilde and Mr. Magnús Lúdvíksson for their help and precious contributions. My grateful thanks go to Ms. Rósa S. Jónsdóttir and Mr. Jóhann F. Kristjánsson for all help in the library and with the computers. In special tribute to our teachers during this course, I would like to express my highest consideration. My thanks and gratitude extend to Reykjavík Geothermal of Iceland for granting access to data.

I would like to express my gratitude to Dr. Maïouf Belhamef, Director of the Center of Development of Renewable Energies of Algeria for support and for granting me permission to attend training at the UNU-GTP. My entire gratitude goes to Dr. Zahia Benaïssa Hameg for

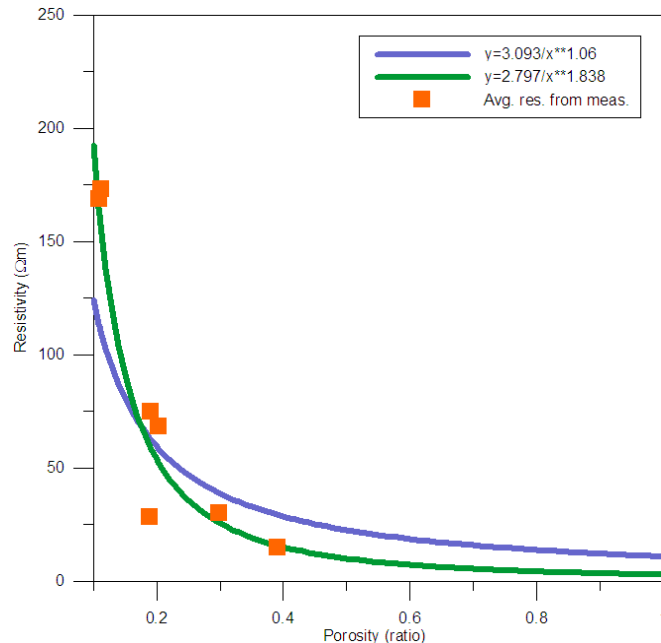


FIGURE 17: Empirical data from Flóvenz et al. (1985) compared to results from well HS-36 where a scale factor 1/100 is used

recommending me for this training and for continuous encouragement. Deepest thanks to my friends, the UNU Fellows and especially the 2009 Fellows, for mutual support over these six months. I dedicate this work to all my teachers.

## REFERENCES

- Axelsson, G., 1991: Reservoir engineering studies of small low-temperature hydrothermal systems in Iceland. *Proceedings of the 16<sup>th</sup> Workshop on Geothermal Reservoir Engineering, Stanford University, California*, 143-149.
- Beardsmore, G.R., Cull, J.P., 2001: *Crustal heat flow - A guide to measurement and modelling*. Cambridge University Press, Cambridge, UK, 324 pp.
- Beck, A. E., 1976: An improved method of computing the thermal conductivity of fluid-filled sedimentary rocks. *Geophysics*, 41-11, 133-144.
- Cermák, V., and Rybach, L., 1982: The thermal conductivity and specific heat of minerals and rocks. In: Angenheister, G. (ed.), *Landolt and Börnstein VII: Physical properties of rocks*. Springer Verlag, Heidelberg-Berlin-NY, 305-344.
- Flóvenz, Ó.G., Georgsson, L.S., and Árnason, K., 1985: Resistivity structure of the upper crust in Iceland. *J. Geophys. Res.*, 90-B12, 10,136-10,150.
- Flóvenz, Ó.G., and Saemundsson, K., 1993: Heat flow and geothermal processes in Iceland. *Tectonophysics* 225, 123-138.
- Fridleifsson, I.B., 1979: Geothermal activity in Iceland. *Jökull*, 29, 47-56.
- Gunnlaugsson, E., and Gíslason, G., 2003: District heating in Reykjavík and electrical production using geothermal energy. *Proceedings of the International Geothermal Congress IGC-2003, Reykjavík*, S11 22-27.
- Hersir, G.P., and Björnsson, A., 1991: *Geophysical exploration for geothermal resources. Principles and applications*. UNU-GTP, Iceland, report 15, 94 pp.
- Rybach, L., 1981: Geothermal systems, conductive heat flow, geothermal anomalies. In: Rybach, L., and Muffler, P.L.J. (eds.), *Geothermal systems: Principles and case histories*. John Wiley & Sons, Ltd, NY, 3-36.
- Serra, O., 1984: *Fundamentals of well log interpretation, Vol. 1: The acquisition of logging data*. Elsevier, Amsterdam, 107 pp.
- Stefánsson, V., 1997: The relationship between thermal conductivity and porosity of rocks. *The Nordic Petroleum Technology III*, 201-219.
- Stefánsson, V., Axelsson, G., and Sigurdsson, Ó., 1982: Resistivity logging of fractured basalt. *Proceedings of the 8<sup>th</sup> Workshop on Geothermal Reservoir Engineering, Stanford University, Ca*, 189-195.
- Stefánsson, V., and Steingrímsson, B.S., 1990: *Geothermal logging I, an introduction to techniques and interpretation* (3<sup>rd</sup> edition). Orkustofnun, Reykjavík, report OS-80017/JHD-09, 117 pp.
- Tómasson, J., 1983: *Well HS-36 in Nauthólsvík, geological logs, alteration, aquifers*. Orkustofnun, Reykjavík, report OS-93067/JHD-33B (in Icelandic), 9 pp.
- Tómasson, J., Fridleifsson, I.B., and Stefánsson, V., 1975: A hydrological model of the flow of thermal water in southwestern Iceland with special references to the Reykir and Reykjavík areas. *Proceedings of 2<sup>nd</sup> UN Symposium on the Development and Use of Geothermal Resources, San Francisco, I*, 643-648.